Materials Science Forum Vols. 196-201 (1995) pp. 1079-1084

DIRECT EXPERIMENTAL EVIDENCE OF AUTOLOCALIZATION NATURE OF DX⁻ CENTERS

S. D. GANICHEV [1,2], I. N. YASSIEVICH [2], W. PRETTL [1], J. DIENER [3], B. K. MEYER [3], AND K. W. BENZ [4]

[1] Institut für Experimentelle und Angewandte Physik, Universität Regensburg, 93040 Regensburg, Germany

[2] A.F. Ioffe Physicotechnical Institute, St. Petersburg, 194021 Russia

[3] Technische Universität München, E16, 85747 Garching, Germany

[4] Kristallographisches Institut, Universität Freiburg, 79104 Freiburg, Germany

Keywords: DX⁻ centers, phonon assisted tunnel ionization, far-infrared radiation.

Abstract. Tunnelling ionization of DX⁻ centers in $Al_xGa_{1-x}Sb$ has been observed in teraher radiation fields. Tunnelling times have been measured for autolocalized and on-site deep impuritie It is shown that in one case the tunneling time is smaller, in the other larger than the reciproc temperature multiplied by a universal constant due to the different tunnelling trajectories. This allov to distinguish in a direct way between the two types of configuration potentials of impurities.

Defect engineering of material properties is one of the key issues of present semiconduct technology. Two remarkable examples of high current interest are the EL2 defect in GaAs [1] ar the DX⁻ center in III-V ternary alloys like AlGaAs, AlGaSb etc. [2-4]. These defects have be studied extensively in the past stimulated by the phenomenon of metastability which both defec have in common. Here we will deal with the DX⁻ center. Shallow n-dopants in ternary III-V allo coexist in two charged states as ionized effective mass like donors and as deep negatively charg DX⁻ centers. By light illumination the DX⁻ center can be made electrically and optically inactive. Tl large difference between optical ε_{opt} and thermal ε_T activation energy and the presence of persiste photoconductivity observed for these centers have been explained by a model of large latti relaxation leading to autolocalization [5,6].

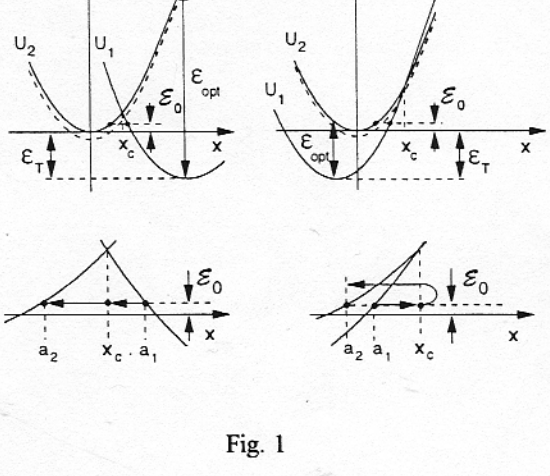

Fig. 1

Fig. 1 presents two adiabati potential diagrams with a shift in th configuration coordinate of th equilibrium position which correspon to electron-phonon coupling wit (Fig. 1 (a)) and without (Fig. 1 (b autolocalization. The configuration Fig. 1 (a) is usually assumed to app to DX⁻ centers giving a big differenc between ε_{opt} and ε_T [2-6]. Th configuration of Fig. 1 (b) correspond to on-site impurities. In this case th difference between ε_{opt} and ε_T usually small but can also be very larg as shown by Henry and Lang [7] f "state 2" oxygen in GaP. The larg difference has been introduced b

taking two different vibrational frequencies for the occupied and the unoccupied state, respectively. The details of the adiabatic potential configuration are of great importance for the non-radiative capture of free carriers.

Here we demonstrate that tunnel ionization in terahertz fields [8-10] allows in a simple way a clear cut distinction between the two types of potential configurations shown in Fig. 1. The tunnelling time, caused by the re-arrangement of the lattice during detachment of the electron, is systematically different for both situations. To be more precise, the tunnelling time is in one case smaller, in the other bigger than the reciprocal temperature multiplied by a universal constant.

Measurements have been carried out on DX^- centers in $Al_xGa_{1-x}Sb$. The results will be compared to ones for on-site impurity gold in germanium. Large electric field strengths have been applied by high-power terahertz radiation. It has been shown previously that the electric field of terahertz radiation acts like a dc field as long as the radiation frequency is smaller than the vibration frequency of the deep impurities [10]. Multiphonon tunnel ionization in strong electric fields has been investigated for various impurities [8, 10]. In Fig. 1 the curves U_1 and U_2 correspond to the ground state and to the ionized center with zero kinetic energy of the charge carrier, respectively. The impurities can be ionized by thermal excitation in the potential U_1 to an energy above the minimum of the ionized configuration U_2 and by tunnelling from the bound configuration U_1 to U_2 [8, 9]. In thermal equilibrium the multiphonon tunnel ionization rate is balanced by the capture of free carriers. In the presence of an electric field E the potential U_2 is shifted to lower energies as a whole (dashed curves in Fig. 1) yielding in semi-classical approximation an excess emission rate [8]

$$e(E) \propto \exp\frac{(eE)^2 \tau_2^3}{3m^*\hbar}, \quad \text{where} \quad \tau_2 = \sqrt{\frac{M}{2}}\int_{a_2}^{x_c}\frac{dx}{\sqrt{U_2(x)-\mathcal{E}_0}}, \tag{1}$$

m^* is the effective mass of free carriers and τ_2 is the tunnelling time [11] along the trajectory from a_2 to x_c (see Fig. 1) in the configuration space under the potential U_2 at the energy $\mathcal{E} = \mathcal{E}_0$. In this relation M is the mass of the defect and $\mathcal{E}_0$ is optimum energy of tunnelling [8, 9]. The energy $\mathcal{E}_0$ decreases with decreasing temperature and approaches the minimum of the potential U_2 in the limit $T \Rightarrow 0$. Thus τ_2 is strongly temperature dependent diverging for $T \Rightarrow 0$.

The temperature dependence of τ_2 may be determined from the condition of optimum tunnelling. As long as the electric field is not to high to change $\mathcal{E}_0$ significantly, τ_2 may be calculated in thermal equilibrium ignoring the electric field. In this case and in the semi-classical approximation the thermal emission rate is given by $P(\mathcal{E}) \propto \exp(-\Psi)$ with $\Psi(\mathcal{E}) = (\varepsilon_T + \mathcal{E})/kT + 2\,|S(\mathcal{E})|$ where $S(\mathcal{E})$ is the principal function multiplied by $i/\hbar$ after [8]. Due to the exponential dependence of $P(\mathcal{E})$ on the energy $\mathcal{E}$, tunnelling takes place at energies in a narrow range around $\mathcal{E} = \mathcal{E}_0$ where $\Psi(\mathcal{E})$ assumes a minimum. After [12, 8] $S(\mathcal{E})$ is to be split into two parts, $S(\mathcal{E}) = -S_1(\mathcal{E}) + S_2(\mathcal{E})$, with

$$S_i(\mathcal{E}) = \frac{\sqrt{2M}}{\hbar}\int_{a_i}^{x_c} dx\sqrt{U_i(x)-\mathcal{E}}, \qquad i = 1,2 \tag{2}$$

This corresponds to tunnelling from a_1 to x_c under the potential U_1 and from x_c to a_2 under potential U_2. These tunnelling trajectories are indicated by arrows on Fig. 1. The condition for finding $\mathcal{E}_0$ is given by

$$\left.\frac{d\Psi}{d\mathcal{E}}\right|_{\mathcal{E}=\mathcal{E}_0} = 2\left.\frac{d|S(\mathcal{E})|}{d\mathcal{E}}\right|_{\mathcal{E}=\mathcal{E}_0} + \frac{1}{kT} = 0\,. \tag{3}$$

The essential difference between the two models discussed here is that $S_1(\mathcal{E})$ and $S_2(\mathcal{E})$ have the same signs for the on-site configuration (Fig. 1 (b)) but the signs are opposite for

autolocalization (Fig. 1 (a)). Thus we have $|S| = |S_1| + |S_2|$ for autolocalization and $|S| = |S_1| - |S_2|$ for the on-site configuration taking into account that $|S_2| > |S_1|$ (see Fig. 1). The magnitude of the derivative $|dS_i/d\mathcal{E}|$ yields the tunnelling times τ_1 and τ_2 along trajectories under the corresponding potentials:

$$\tau_i = \hbar \left| \frac{dS_i}{d\mathcal{E}} \right|_{\mathcal{E}=\mathcal{E}_0} \qquad i = 1,2 . \qquad (4)$$

From Eqs. (3) and (4) we find

$$\tau_2 = \frac{\hbar}{2kT} \pm \tau_1 \qquad (6)$$

where the minus and plus signs correspond to Fig. 1 (a) and (b), respectively. As $\mathcal{E}_0$ is much larger than the minimum of U_1, τ_1 is approximately the period of oscillations in U_1 and does not significantly depend on temperature and electric field. For on-site deep impurities like Au, Hg, Zn, Cu in germanium it has been shown that τ_2 is larger than $\hbar/2k_BT$ and follows the temperature dependence of Eq. (6) [8, 10]. For autolocalized states τ_2 is expected to be smaller than $\hbar/2k_BT$.

The investigations of phonon assisted tunnelling have been carried out on $Al_xGa_{1-x}Sb$ samples grown by the travelling heater method from Sb rich melts. Tellurium was added into the melt resulting in n-type conduction ($n = 4 \cdot 10^{17}$ cm^{-3}). The crystals were characterized by Hall effect measurements, deep level transient spectroscopy (DLTS) and photocapacitance measurements. All the essential features of the DX^- centers, in particular persistence photoconductivity, have been observed. The actual sample compositions were x = 0.28 and 0.5. More details of the properties of the samples can be found in [13, 14]. The radiation source used was a pulsed far-infrared molecular laser optically pumped by a TEA CO_2 laser. Using NH_3 and D_2O as active gases, 40 ns pulses with a peak power of 100 kW have been obtained at wavelengths, λ, of 90.5 μm, 152 μm and 250 μm. The $Al_xGa_{1-x}Sb$ samples were placed in the dark in a temperature variable optical cryostat. Measurements have been carried out in the temperature range between 40 K and 90 K where the impurity centers are occupied in thermal equilibrium.

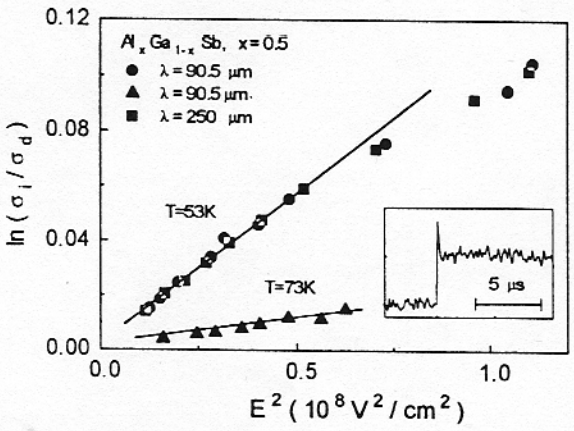

Fig.2

The photoconductive signal strongly nonlinear with the radiation intensity has been observed at all wavelength and temperatures. The signals consist of two components (see inset of Fig. 2), a fast one with decay time of about 80 ns and a long tail which did not decay within the presented time scale of Fig. 2. Measurements of the radiation induced conductivity change of the sample by a dc voltmeter have shown that this part of the signal persists for several hundreds of seconds which corresponds to the life time of persistent photoconductivity observed for DX^- centers in investigated samples [13,14]. The sign of the photoconductive signal indicates a decrease in the sample resistance and, thus, to an increase in the free carrier concentration. The observation of a positive persistent photoconductivity shows that this signal is caused by the detachment of electrons from

DX^- centers . The fast component of the signal can be attributed to ionization of native Ga acceptor [15] or μ-photoconductivity due to electron heating and is not of interest for the present work. Because of the large difference in relaxation time, the signals may easily be distinguished and investigated at the same time. All data will further be related just to the slow component of the signal. Fig. 2 shows the dependence of $\ln(\sigma_i/\sigma_d)$ on the square of the amplitude of the optical electric field for two different wavelengths and temperatures, where σ_d and σ_i are the dark and irradiation induced conductivities of the sample, respectively. As the duration of the light pulses is much shorter than the capture time of nonequilibrium carriers, recombination may be ignored during excitation. Therefore the experimentally determined relative change in photoconductivity, $\Delta\sigma/\sigma$, is equal to $\Delta n/n$ where n is the free carrier concentration. In Fig. 2 it is seen that the probability of photoexcitation $e(E)/e_0=\sigma_i/\sigma_d$ depends on the electric field as $\exp(E^2/E^2_c)$. The magnitude of the characteristic field E_c does not depend on the wavelength in the present spectral range between 90.5 μm and 250 μm but it is significantly lower for lower temperatures. As it has been shown in [10] this observation rules out other mechanisms of nonlinear optical carrier generation like multiphoton transitions [16, 17] light impact ionization [18], photon assisted tunnelling [19] which all show a characteristic wavelength dependence. The fact that the photoconductivity is independent on the wavelength, the exponential dependence of σ_i/σ_d on the square of the electric field of the radiation and the variation of the signal with temperature permit to conclude that free carriers are generated by phonon assisted tunnel ionization of DX^- centers with far infrared radiation. As it is seen from Fig. 2, at high field strengths the ionization probability increases slower than $\exp(E^2/E^2_c)$ with rising electric field, E_c. Such a behaviour may be attributed to a transition of the ionization process from phonon assisted tunnelling to direct tunnelling in agreement with theoretical [8, 9] and experimental results [20].

The tunnelling time τ_2 is calculated as a function of temperature from the experimental determined square of characteristic field $E^2_c = (3m^*\hbar)/(e^2\tau_2^3)$ which is taken from (1). In Fig. 3 τ_2 of DX^- center in $Al_xGa_{1-x}Sb$, x=0.5 is plotted versus the reciprocal temperature 1/T. For the purpose of comparison Fig. 3 contains also a $\hbar/2kT$ curve and the tunnelling time τ_2 of the on-site deep acceptors gold in germanium (binding energy 150 meV, configuration Fig. 1 (b)), which we measured by the same method. In both cases τ_2 is of the order of $\hbar/2kT$ and follows the 1/T temperature dependence. The representation of Fig. 3 unambiguously demonstrates that τ_2 is larger than $\hbar/2kT$ for an on-site impurity, however, it is smaller than $\hbar/2kT$ for the DX^- centers. This result clearly proves that the autolocalized and on-site impurities may be distinguished by the tunnelling time being determined from phonon assisted tunnelling in terahertz fields. Even small change in τ_2 may be resolved because the emission probability depends exponentially on the third power of the tunnelling time. The tunnelling time reflects the structure of the potential barriers which are systematically distinct for both potential configurations discussed here.

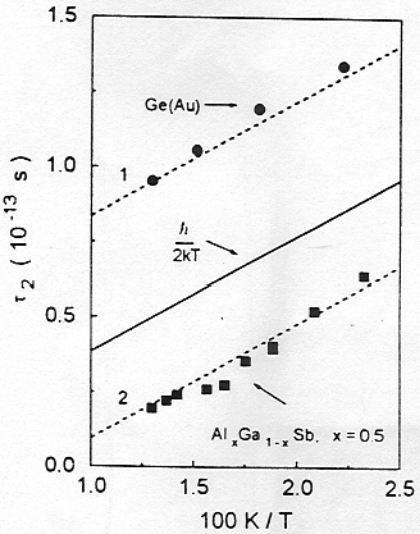

Fig. 3

In summary, photoionization of deep impurity centers in semiconductors has been investigated by high-power pulsed far-infrared laser with quantum energies of the radiation much smaller than the impurity ionization energy. A photoconductive signal increasing nonlinearly with rising incident power has been observed for autolocalized DX^- centers in $Al_X Ga_{1-X}Sb$ and various deep on-site acceptors in Ge. As an important result, the signal strength at given temperature has been found to be independent of far-infrared radiation frequency suggesting that the signal is caused by electric field ionization. In a substantial range of electric field strengths the emission probability of carriers could be attributed to phonon assisted tunneling. The thermal emission of carriers from the impurity bound state into the continuum is usually accomplished by thermal activation of the system in the adiabatic bound state potential and tunneling of the bound defect configuration into the ionized configuration. An electric field enhances defect tunneling due to electron tunneling through the barrier formed by the electron potential and the electric field. This increase in emission of carriers has been detected as photoconductive signal. The electric field dependence of the observed signal allowed to determine defect tunneling times. It has been shown that, due to different tunneling trajectories, on-site impurities and autolocalized centers may unambiguously be distinguished by the value of the tunneling time compared to the reciprocal temperature multiplied by universal constants.

Acknowledgement. Financial support by the Deutsche Forschungsgemeinschaft is gratefully acknowledged.

References

[1] G. M. Martin, S. Makram-Ebeid, in Deep centers in semiconductors, edited by S. T. Pantelides (Gordon and Breach Science Publisher, New York, 1986).
[2] P. M. Mooney, J. Appl. Phys. **67**, R1 (1990).
[3] P. M. Mooney and T. N. Theis, Comments Cond. Mat. Phys. **16**, 167 (1992).
[4] R. C. Newman, Semicond. Sci. Tecnol. **9**, 1749 (1994).
[5] D. V. Lang and R. A. Logan, Phys. Rev. Lett. **39**, 635 (1977).
[6] D. V. Lang, R. A. Logan and M. Jaros, Phys. Rev. B **19**, 1015 (1979).
[7] C. H. Henry and D. V. Lang,Phys. Rev. B **15**, 989 (1977).
[8] V. Karpus and V. I. Perel, Sov. Phys. JETP **64**, 1376 (1986).
[9] V. N. Abakumov, V. I. Perel, and I. N. Yassievich, *Nonradiative Recombinationin Semiconductors*, edited by V. M. Agranovich and A. A. Maradudin, Modern Problems in Condensed Matter Sciences Vol. 33 (North Holland, Amsterdam, 1991).
[10] S. D. Ganichev, W. Prettl, and P. G. Huggard, Phys. Rev. Lett. **71**, 3882 (1993).
[11] Landauer and Th. Martin, Rev. of Mod. Phys. **66**, 217 (1994).
[12] L. D. Landau and E. M. Livshitz, Quantum Mechanics (Pergamon, Oxford, 1977), p. 185.
[13] B. K. Meyer, G. Bischopink, K. W. Benz, A. Schöner, and G. Pensl, J. of Crystal Growth **128**, 475 (1993).
[14] R. Krause-Rehberg, Th. Drost, A. Polity, G. Roos, G. Pensl, D. Volm, B. K. Meyer, G. Bischopink, and K. W. Benz, Phys. Rev. B. **48**, 11723 (1993).
[15] W. Rühle, W. Jakowetz, and M. Pilkuhn, in *Luminescence of crystals molecules and solutions*, edited by F. Williams (Plenum Press, New York, 1973). p.444.
[16] L. V. Keldysh, Sov. Phys. JETP **20**, 1307 (1965).
[17] W. Böhm, E. Ettlinger, and W. Prettl, Phys. Rev. Lett. **47**, 1198 (1981).
[18] S. D. Ganichev, S. A. Emel'yanov, A. P. Dmitriev, Ya. V. Terent'ev, I. D. Yaroshetskii, and I. N. Yassievich, Sov.Phys. JETP **63**, 256 (1986).
[19] P. S. S. Guimaraes, B. J. Keay, J. P. Kaminski, S. J. Allen, P. F. Hopkins, A. C. Gossard, L. T. Florez, and J. P. Harbinson, Phys. Rev. Lett. **70**, 3792 (1993).
[20] S. D. Ganichev, J. Diener, and W. Prettl, Solid State Comm. **92**, 883 (1994)